Analyst

PERSPECTIVE

View Article Online
View Journal

Cite this: DOI: 10.1039/d5an01351h

Opportunities and challenges for analytical chemists: organ-on-chip devices as new approach methods (NAMs) for identifying potential toxins

Evan Huang,[a] Jose A. Nolasco,[a] Sarina J. Jones [a] and Matthew R. Lockett *[a,b]

Received 22nd December 2025,
Accepted 29th May 2026

DOI: 10.1039/d5an01351h

rsc.li/analyst

New approach methodologies (NAMs) integrate and leverage *in vitro* and *in silico* methods to predict human responses to new chemical entities (NCEs). Organ-on-chip (OoC) devices represent advanced *in vitro* models that best model organ-level function. The current rate of device innovation far outpaces the integration of these devices into existing workflows, which rely on monolayer cultures and animal models that have both proven poor predictors of NCE toxicity in humans. This perspective highlights the criteria we believe are needed for OoC devices to meet the biological and technical requirements for increased predictive power and reproducibility in current tissue culture laboratories: anatomically relevant structures that incorporate extracellular matrices and cellular compartmentalization, continuous perfusion for prolonged studies, and designs capable of collecting scalable amounts of sample material for quantitative analyses. Specifically, we focus on advances in readily accessible fabrication and analysis methods that are making OoC models a tractable solution for tissue culture laboratories as they move from monolayer cultures to more sophisticated models. We argue that OoC device adoption is limited not by biological relevance but by a lack of standardized regulatory benchmarks and insufficient compatibility with existing experimental workflows.

The Food and Drug Administration (FDA) Modernization Act 2.0 marked a major shift in how new chemical entities (NCEs) are evaluated in the United States.[1] This bill authorized the replacement of animal testing with new approach methodologies (NAMs), including *in vitro* and *in silico* tools that predict human responses to NCEs, whether they are drug candidates or potential toxins. *In vitro* NAMs range from single-cell assays to three-dimensional culture formats that incorporate the structure and complexity of human tissues or organs. Monolayer cell cultures, maintained in well-plate formats, are the current workhorse for evaluating toxicity and mechanism of action. The need to innovate and refine this approach is clear, with 30% of drug candidates causing organ-specific toxicities in clinical trials or after release to the market.[2,3] These toxicities were neither detected nor predicted in cell-based assays or animal models. Liver toxicity is the primary cause of post-market approval withdrawals,[4] further highlighting that current pre-clinical models cannot predict idiosyncratic responses that become apparent after post-market release. For perspective, the average cost of bringing a single small molecule to market from 2000 to 2018 was $879 million, with 20% of these costs attributed to successful candidates.[5]

There is ongoing effort to develop *in vitro* testing platforms capable of maintaining organ-relevant cellular microenvironments and of simulating the strength and duration of NCE exposure. Analytical chemists have been the nexus of the NAMs effort, developing the (bio)chemical analyses, microfabricated devices, and instrumental advances needed to analyze cellular responses to NCEs in tissue and organ-like structures. Early examples of 3D cultures that better predicted tumor responses to chemo- and radiation therapies were spheroids,[6,7] first described by Sutherland in the 1970s. These models were expanded by pioneers such as Mina Bissell,[8–10] who recognized that cellular responses are context-dependent. Spheroids and organoids are three-dimensional architectures that can recapitulate the structure and function of an organ.[11–13] Spheroids are assemblies of differentiated cells, whose composition and organization are dictated by the end user. Hepatocyte-only spheroids have proven superior to their monolayer analogs for maintaining key metabolic pathways that were otherwise dysregulated in 2D cultures.[14,15] Organoids originate from stem-like cell types, differentiated to form a self-assembled structure that contains the cell type(s) found in the organ of interest. Organoids can be patient-specific, derived from induced pluripotent stem cells (iPSCs). These iPSCs are collected from an

[a]*Department of Chemistry, University of North Carolina at Chapel Hill, Chapel Hill, NC 27599-3290, USA. E-mail: mlockett@unc.edu*
[b]*Lineberger Comprehensive Cancer Center, University of North Carolina at Chapel Hill, Chapel Hill, NC 27599-7295, USA*

individual, dedifferentiated through standard culture practices and maintained as monolayers until needed. Through a series of chemical treatments, the iPSCs can be differentiated into a tissue or organ of choice that contains the exact DNA sequence as the patient. However, despite their improvements upon 2D monolayer cultures, spheroids and organoids represent the more primitive side of 3D culture formats. The reproducibility of spheroid geometry and size can be limited when relying on spontaneous formation from methods such as hanging drops and spinner flasks. These methods also result in low throughput and more labor-intensive analysis.[16,17] These challenges sparked the growing interest in microfluidics as a possible solution.

Organ-on-chip (OoC) devices are advanced *in vitro* NAMs. These devices support anatomically relevant structures and physiologies that mimic the tissues or organs they are designed to emulate. Since the first reported cell-containing microfluidic channels, many innovative device designs, cell culture methods, analyses, and cell collection methods have emerged. A notable early example is the lung-on-a-chip model described by Huh and Ingber.[18] This two-chamber device used a flexible, porous PDMS membrane to separate alveolar epithelial and endothelial cells. To mimic breathing, the membrane was stretched at a lung-like frequency. In the past fifteen years, OoC devices have expanded to model the blood–brain barrier, gut, kidney, liver, and immune system.[19–24]

This perspective focuses on advances in fabrication and analysis that make OoC models a tractable solution for predicting human responses to NCEs. To organize the presentation, we focus on three facets needed to generate physiologically relevant models: anatomical structures that incorporate extracellular matrices and cellular compartmentalization, continuous perfusion of cells throughout prolonged experiments, and designs that are easily scalable to collect sample sizes needed for endpoint and -omic analyses. With an eye toward the near future, we focus on efforts that use readily accessible materials and fabrication methods to achieve tissue- and organ-level responses that match those of advanced fabrication methods, which may require engineering expertise. Our research endeavors focus on effective low-cost devices, enabling researchers to prioritize repeatability without the financial or technical costs of adopting entirely new workflows. Culture platforms that rely on existing analysis protocols enable data harmonization and direct comparison with previous monolayer cultures.

Beyond the monolayer: analytical challenges of fabricating and measuring cellular responses in tissue- and organ-like structures

In 1910, Harrison documented the maturation of neurons in embryonic frog tissues maintained in hanging droplets.[25] A year later, Carrel described the prototype of the modern culture flask.[26] The first immortalized cell line maintained as a monolayer was obtained from Henrietta Lacks in the 1950s, unbeknownst to her.[27] Despite well-established protocols and standardized equipment for preparing and maintaining monolayer cultures of immortalized cell lines, recent meta-analyses of prior results highlight the difficulty of achieving intra- and interlaboratory reproducibility.[28,29] Seemingly minor changes in tissue culture practices between researchers can cause major variations in cellular phenotype and response. The current practice of publishing common incubator settings (*e.g.*, 37 °C, a 5% CO_2 gas composition, resulting humidity) and defined culture medium compositions is not enough to ensure reproducible datasets. What is needed is a more stringent set of guidelines for the maintenance and evaluation of cellular responses to NCEs, similar to the Minimal Information for Quantitative Real-Time PCR Experiments (MIQE) framework.[30,31] Riss proposes such an effort for cell culture laboratories, treating cells as reagents whose maintenance and culture conditions are highly controlled.[32]

Cell culture-compatible microfabricated devices are a natural extension of the micro-total analytical systems (μTAS), which reduce laboratory-scale operations to a few milliliters of reagents. These devices also increase experimental repeatability by automating sample preparation and analysis. Furthermore, working in micron-scale channels provides greater control over reagent delivery than well plates, due to the laminar flow profiles at these scales. Building on these advantages, OoC devices place cells in defined architectures that approach the complexity of the generalized epithelial tissue shown in Fig. 1. In these devices, cell types are arranged in a three-dimensional architecture to maintain tissue function. Each cell type is supported by an extracellular matrix (ECM) of a particular composition and viscoelasticity. The cell types do not function autonomously but rather work in harmony through a temporally dynamic signaling system composed of biomolecules.

Fabrication and measurement challenges are inherent to any cell-based assay. These issues must be carefully considered and rigorously evaluated before extrapolating *in vitro* results to human-level responses. Fabrication challenges include designing anatomically relevant structures that incorporate length scales, extracellular matrices, and cell types. Measurement challenges go beyond basic characterization before and after exposure to an NCE. Endpoint analyses of viability are often used to determine dose–response relationships to quantify toxicity. There are numerous stains and commercial assays for quantifying cellular viability; many are optimized for monolayer culture in well plates and require careful consideration and adjustment when applied to cells maintained in 3D environments, which contributes to variability between labs.[33] Detailed spatial and temporal views of the microenvironment are needed to assess sources of heterogeneity. Real-time measurements of extracellular oxygen, pH, and glucose are necessary to attribute differences in NCE exposure to biological variation rather than to changes in experimental conditions. Such sensors, including those we and others have

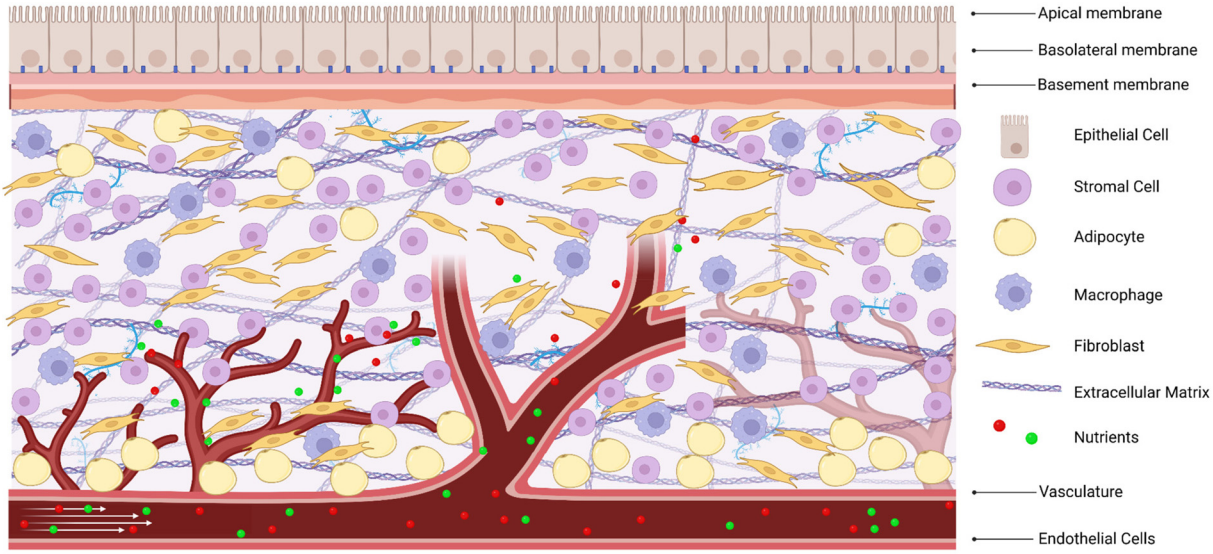

Fig. 1 Schematic of a generalized epithelial barrier, defined by a basement membrane that separates polarized epithelial cells from stromal cell types suspended in an ECM. The vasculature supplies these cells with nutrients and oxygen, while also removing unwanted waste products. This figure was generated with BioRender.com and is for illustrative purposes of the tissue microenvironment. The scaling of this schematic is neither accurate nor uniform.

described, can be readily incorporated into 3D cultures and microfabricated devices.[34–38]

To illustrate the challenges in measuring a concentration-dependent response in a two-component co-culture, consider an epithelial cell type separated from fibroblasts by an ECM. Although our approach may seem obvious, it warrants review given the many variables that affect cellular responses. For example, individual dose–response relationships of each cell type (as monocultures) are needed to assess toxicity. In these experiments, parameters such as cell density and ECM composition must be evaluated to ensure a sufficiently high signal-to-background ratio, with background responses arising from the vehicle control. Notably, cell density can affect experimental outcomes, as pericellular hypoxia is often overlooked. Furthermore, NCEs can influence glucose metabolism and acidify the medium during an experiment. While a single time point is chosen for these studies, time-course measurements are necessary to determine the optimal assay time, since not all NCEs cause toxicity *via* the same mechanism.

In co-culture formats, changes in cell cycle and morphology must also be tracked. Here again, characterization of the microenvironment is needed if the co-culture differs from the monocultures in cell density, configuration, or culture medium. Finally, the dose–response relationship of the co-culture must be measured carefully to ensure that the epithelial and fibroblast components can be quantified independently. The myriad consequences of small adjustments to the cellular microenvironment require evaluation across many users, while incorporating design aspects that minimize variability to what is biologically relevant. Below, we define and highlight key components of the future of organ-on-chips essential for maintaining physiological relevance and analytical rigor.

Goal 1. Anatomically relevant tissue structures

Fig. 1 depicts a generalized epithelial barrier and highlights the differences between the epithelial and stromal components. Epithelial cells are highly organized. These polarized cells form a barrier through protein-enabled tight junctions. Stromal cells are less organized than epithelial cells. They maintain tissue integrity and repair wounds, two aspects of homeostasis that favor a dynamic environment capable of readily changing cellular organization and density as needed. In microfabricated devices, different cell types are often separated by extracellular matrices (ECMs)[39] or porous polymeric sheets that serve as artificial barriers. Transwell assays commonly use porous polyethylene terephthalate (PET) or polycarbonate (PC) films to separate epithelial and stromal cells, much like the proteinaceous basement membrane shown in Fig. 1. This two-compartment format has been used to model the blood–brain barrier, quantify cellular invasion and intravasation, and quantify nuclear receptor transactivation.[40–45] A limitation of this setup is its inability to maintain a chemical gradient across the membrane for prolonged periods, to support real-time analysis, and to promote spatial cell organization.

Awe-inspiring devices supporting organ-like structures are published monthly. These advances in fabrication techniques enable the integration of multiple cell types into anatomically relevant architectures. Fig. 2 highlights recent examples of

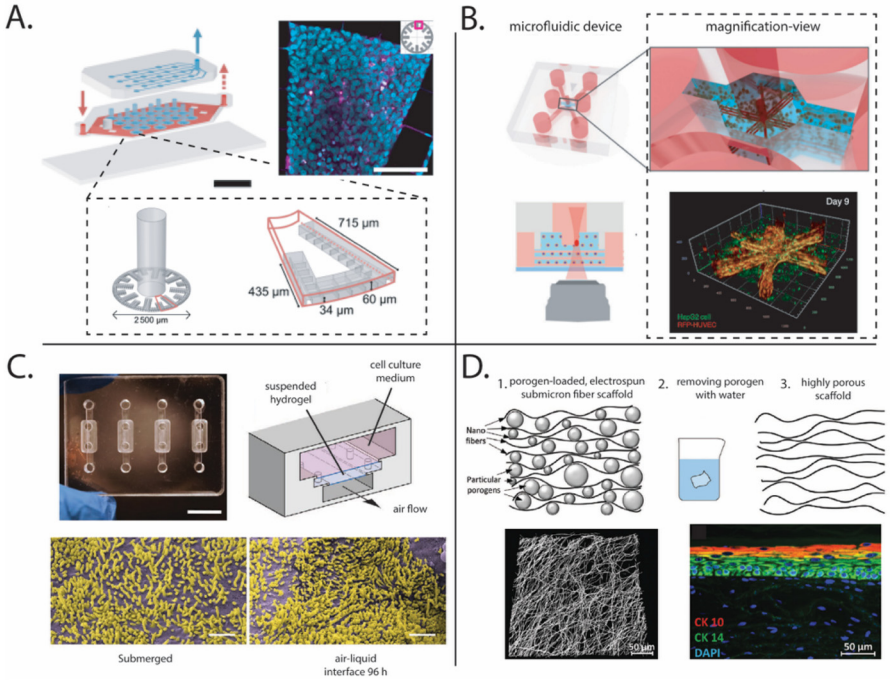

Fig. 2 Architecturally relevant tissue and organ structures. (A) A two-layer PDMS liver lobule device in which culture medium flows through 16 chimney-like structures. Sinusoid-like structures surround the 60 μm tall chimneys and support hepatocytes in a basement membrane extract (Geltrex). The fluorescence micrograph contains Hoechst-stained cells (scale bar = 100 μm). Adapted from ref. 46, copyright 2025, with permission from the RSC. (B) A liver lobule structure with an interconnected microvascular network, generated directly in the cell-containing hydrogel with a high-definition laser patterning technique. Adapted from ref. 47, copyright 2024, with permission from Elsevier. Once formed, the inner walls of the microvascular network were lined with endothelial cells. A confocal fluorescence image of the device, nine days after seeding with HUVECs (cube = 1200 × 1200 × 400 μm). (C) An air–liquid interface culture prepared from suspending a lung adenocarcinoma-lined hydrogel between two micro-milled PMMA pieces. Adapted from ref. 48, copyright 2021, with permission from Wiley. The number of cilia-like projections formed in the device, expected in polarized lung epithelial cells, increased when transitioning from static (submerged) to perfused (ALI) experimental conditions. These cilia are apparent in the SEM image (scale bar = 1 μm). (D) Highly porous scaffolds prepared by electrospinning nylon-6 or poly(ε-caprolactone) containing water-soluble porogens. When stacked, scaffolds seeded with either keratinocytes or fibroblasts form a functional epidermis that supports ECM deposition, homogeneous distribution of fibroblasts throughout the stromal layers, and the development of a differentiated epidermal layer. Adapted from ref. 49, copyright 2022, with permission from Wiley.

devices prepared with advanced fabrication techniques. It also contains comparable devices, prepared with components more readily accessible to biologically focused tissue culture laboratories. Dalsbecker prepared an array of 21 sinusoids using perforated walls to separate hepatocyte-containing regions from a medium reservoir (Fig. 2A).[46] Watanabe used a top-down approach and formed tubular structures (20–30 μm in diameter) directly in a hepatocyte-containing hydrogel (Fig. 2B).[47] These structures were formed using a high-definition laser patterning technique with a photo-crosslinked diazosulphonate resin, coated with HUVECs to form a functional vasculature network. In a more readily adopted approach, Park used a desktop milling machine to prepare PMMA pieces, which were assembled around a preformed hydrogel slab (Fig. 2C).[48] One side of the hydrogel slab was lined with lung adenocarcinoma cells to form an air–liquid interface for assessing lung function. The hydrogel could also be easily removed from the device for post-experimental analyses. Weigel formed scaffolds by electrospinning nylon or poly(ε-caprolactone) in the presence of NaCl porogens (Fig. 2D).[49] After salt removal, the remaining porous scaffolds were seeded with cell-laden hydrogels. In one example, a two-layered skin model was prepared using scaffolds seeded with human dermal fibroblasts and epithelial keratinocytes.

Goal 2. Continuous perfusion to maintain and evaluate functional tissue and organ microenvironments

The vasculature included in Fig. 1 is the primary site for nutrient and waste exchange in tissues. In well-innervated epithelial tissues, the microvasculature network has a vessel every 100 mm.[50] Even with frequent medium exchanges, monolayer cultures are subject to oxygen stress under static culture conditions.[51,52] Pericellular hypoxia, or an insufficient oxygen concentration around cells, results when cellular oxygen consumption outpaces diffusion. Limited oxygen triggers cellular reprogramming, which is coordinated by hypoxia-inducible factors.[53,54] These transcription factors are the master regula-

tors of cellular metabolism and apoptosis. Insufficient oxygen also causes rapid acidification of the medium, as cells now rely on glycolysis, leading to lactic acid release.[55,56] Spheroids, organoids, and cell-laden scaffolds are more prone to pericellular hypoxia than monolayer cultures, as not all cells are in direct contact with the medium. Optical and electrochemical oxygen sensors integrated directly into microfabricated devices rapidly detect hypoxic microenvironments across all culture conditions, including OoC devices.[34,36,57]

To address these challenges, *in vitro* devices use oxygen-permeable materials and continuous medium exchange to mitigate hypoxia. Early devices featured elastomers like PDMS,[58] which support cells in well-oxygenated environments but absorb hydrophobic molecules. More recent devices use silicone-based hydrogels and thermoplastics.[59–61] Continuous-flow systems have adjustable flow rates that ensure medium exchange, overcoming pericellular hypoxia and removing waste. The microliter-per-minute-or-less exchange rates in microfabricated devices ensure that the total volume consumed over a multi-day experiment is less than that of traditional static cultures in well plates. An additional consideration with these devices is that the shear stresses associated with the flow of a medium through confined spaces can affect cellular responses. Early microfluidic device studies showed that shear stress controls cellular health and cell adhesion.[62] Shear stresses help maintain endothelial cell integrity and support the integrity of healthy stromal and epithelial tissue components.[63–66] For example, shear stress affects the alignment, polarity, and migration of fibroblasts within channels.[67,68] It also dictates endothelial cell health, which is influenced by hemodynamic forces as blood flows.[69] Liquid exchange in microfabricated devices is achieved through tubed or tubeless systems. Tubeless systems offer less control than

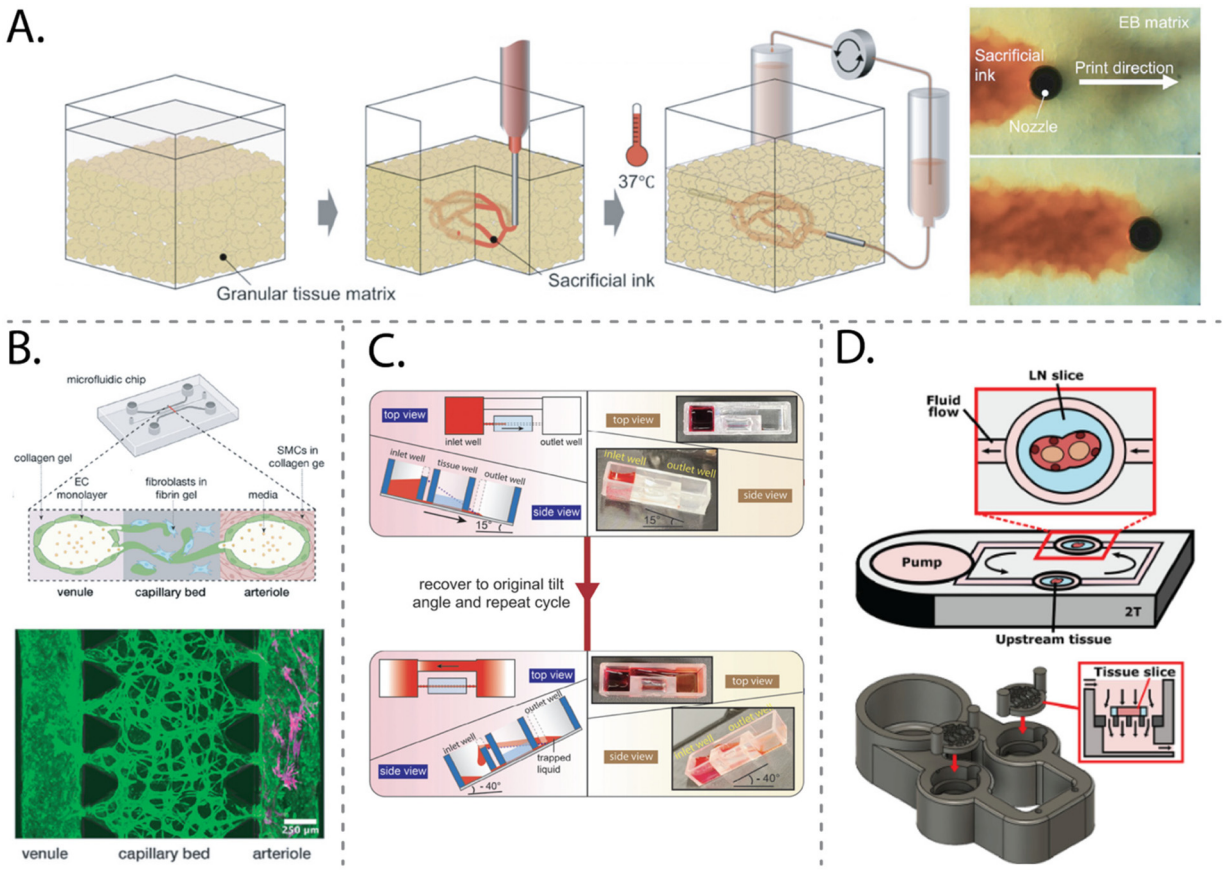

Fig. 3 Continuously perfused systems supply oxygen and nutrients to tissue- or organ-like structures. (A) Vessel-like structures were extrusion-printed into a liquid granular tissue matrix using gelatin-based sacrificial inks. The ink remained solid during deposition at 4 °C and then liquified at the 37 °C needed to maintain the ECM. After the liquid was removed, the microtubules were lined with endothelial cells. Adapted from ref. 73, copyright 2019, with permission from AAAS. (B) A device that enabled natural capillary bed formation in a fibrin slab situated between two endothelial-lined vessel structures. The vessels were maintained under culture conditions that mimic arteriole and venule flow and microenvironments. Adapted from ref. 74, copyright 2023, with permission from the RSC. (C) A three-component device that promotes unidirectional flow of culture medium through a central cell-containing well using a tabletop rocker. When held at a low angle (15°), medium flows from the inlet well to the outlet well through a gelatin slab. When held in the opposite direction (–40°), the medium flows from the outlet well to the inlet well through a channel that bypasses the cell-containing well. Adapted from ref. 70, copyright 2023, with permission from Wiley. (D) An all-in-one 3D-printed device that uses magnetic stir bars to circulate culture medium in a closed-loop system. The medium circulates from a reservoir through two units, each containing a tissue slice. Adapted from ref. 76, copyright 76, with permission from the RSC.

those plumbed with inlet and outlet tubing but are easier to implement in tissue culture laboratories. Tabletop rockers readily move liquids in tissue culture flasks or well plates,[70] but this gravity-based exchange doesn't work in micron-sized channels due to high flow resistance. Increasing channel dimensions to the millimeter scale lowers resistance and allows rocker use.[71,72]

Fig. 3 contains four recent examples of perfusable OoC devices. Skylar-Scott used extrusion-based printing to insert sacrificial gelatin ink into centimeter-thick ECM that contained embryoid bodies, cerebral organoids, or cardiac spheroids (Fig. 3A).[73] Under chilled conditions, the ECM accommodated the gelatin ink, deposited through a 1 mm-diameter nozzle. When warmed to 37 °C, the ECM stiffened, and the melted gelatin was removed to reveal hollow vessels. These vessels were lined with endothelial cells and then perfused with culture medium. Chen formed a perfusable microcapillary network between two endothelial-lined vessel structures, maintained within an arterial or venous microenvironment (Fig. 3B).[74] The vessel structures were generated with viscous finger molding and separated by a fibrin gel slab. A functional microvascular network formed naturally within the fibrin matrix, connecting the two vessels. Zhang fabricated a pumpless recirculating device by attaching a section of a bottomless well plate to an adhesive sheet (Fig. 3C).[70] Recirculation was achieved through tilting of the device. Tilting in one direction drew culture medium through the cell-containing well and along a gelatin strip that connected the inlet and outlet wells. Tilting the other way, let the medium bypass the cell-containing well *via* a connecting channel. Pompano designed a 3D-printed device (Fig. 3D) that contained magnetic stir bars. The stir bars functioned as impellers, recirculating culture medium over tissue slices.[75,76] This setup enabled studies of intercellular communication, specifically inter-organ signaling with lymph nodes. Using a single printed component for fluid delivery eliminated the need for tubing and fittings prone to bubble formation and occlusion.

Goal 3. Ease of sample collection and scale-up for quantitative measurements of cellular responses

Despite many excellent examples of real-time and endpoint analyses of OoC devices, there remains a disconnect between the number of cells a device can support and those needed for routine cellular analyses. Microfabricated devices have excelled in optical methods because they are generated from transparent materials compatible with fluorescence microscopy and high-content imaging. Confocal microscopy can achieve axial resolutions of 0.5–20 μm, allowing for segmented analysis of the entire microfluidic channel 10–20 μm in height. The small number of cells or the pL–μL volumes of liquid that can be collected from a microfluidic channel can pose challenges for commonly used analytical readouts, as summarized in Table 1. For example, a close-packed assembly of spherical MCF7 cells (20 μm in diameter) in a 1 mm × 20 mm channel monolayer contains approximately 6.3×10^4 cells. This number of cells corresponds to 1.9 μg of total RNA and 6.3 μg of total protein, assuming 30 pg of RNA and 100 pg of protein per cell. Techniques that require larger sample inputs are where microfabricated devices cannot compete with traditional monolayer culture formats, as scale-up requires (1) re-engineering and fabrication steps or (2) the pooling of samples collected from multiple devices. To reach the 2.0×10^6 MCF7 cells needed for a successful flow-sorting experiment, the above channel would need to be at least 10 mm tall, closer to 20 mm if the cells were suspended in an equal volume of ECM. These dimensions are not feasible by current standards, where a typical channel has a 10 : 1 width-to-height ratio. Individuals have developed channels with lengths ranging from 10–100 cm, a design feature commonly used in microchip separations.[77,78] To compensate for the limited sample in a single device, the contents of several devices are combined. Pooled datasets have two drawbacks. First, individual responses within a device can

Table 1 Inputs needed for common targeted and discovery-based analyses

	ELISA[a]	RT-qPCR[b]	SIMOA[a]	Flow cytometry[c]	RNA sequencing[d]	Proteomics[e]	Metabolomics[f]
Analytical modality	Colorimetric	Fluorescence	Fluorescence	Fluorescence	Fluorescence	*m*/*z* ratio	*m*/*z* ratio
Instrument	Plate reader	qPCR machine	Dedicated instrument	Cytometer or FACS	RNA Sequencer	LC-MS/MS	LC-MS/MS
Sample volume	100 μL	10–25 μL	100 μL	Single cell suspension	10–25 μL	<10 μL	<10 μL
Sample requirement	pg–ng total protein	ng–μg total cDNA	fg–pg total protein	$0.5–2.0 \times 10^6$ cells	ng–μg total cDNA	pg–μg total protein	Cell lysate ($0.5–2.0 \times 10^6$ cells)
Cost[g]	$	$	$$	$$$	$$$	$$	$$

[a] Values estimated from a commercial vendor source for a sandwich ELISA format with an HRP colorimetric readout; type of ELISA and a Quanterix SR-X instrument (source: https://www.raybiotech.com). [b] Values estimated from commercial vendor websites and ref. 82. [c] Values estimated based on commercial vendor sources. [d] Values from the National Cancer Institute Bioinformatics Training and Education Program.[83] [e] Values estimated for an Orbitrap Exploris 480 mass spectrometer, analyzing HeLa cell lysate. [f] Values estimated for a Q Exactive HF Orbitrap mass spectrometer, analyzing tricarboxylic acid (TCA) cycle metabolites from UM1, UM2, UMSCC5, and UMSCC6 cancer cells. [g] Cost estimations per sample analyzed. $: 1–10 $$: 20–50 $$$: 100–200. Based on a per sample cost.

be lost. Second, the dataset's robustness is reduced because several potential datasets are collapsed into a single average.

OoC devices compatible with existing workflows for NCE screening and evaluation are less daunting than those needing specialized equipment or unfamiliar assays. The analytical techniques in Table 1 provide average cellular responses to NCEs, relying on analyte enrichment or signal amplification strategies to bridge the gap between what is measurable and what is present in cellular lysate. Analyte enrichment improves the signal-to-background ratio of a measurement by removing interferences and increasing analyte concentration. Immunocapture and RNA purification are examples of analyte enrichment. Chromatographic separation prior to MS-based analysis is a common analyte enrichment strategy for complex mixtures. Signal amplification ensures that analytes below the assay's limit of detection can be detected and quantified; in some instances, analyte enrichment is needed before signal amplification to remove interferences. The signal amplification of enzyme-based readouts used in immunoassays has enabled the detection of proteins at picogram levels with enzyme-linked immunosorbent assay (ELISA) and at femtogram levels with the recently developed single-molecule array (SIMOA) platform.[79,80] ELISAs are a mainstay for targeted protein quantitation, with samples analyzed for multiple analytes in one or multiple wells. The current Quanterix SIMOA platform offers a 10-plex analysis from a single sample. The polymerase enzymes are also a staple of molecular biology, quantifying genome-wide expression *via* sequencing or targeted gene expression through analog or digital readouts. Procedures for lysing cells in a microfluidic channel are well established,[81] but they limit spatial analysis because all cellular contents exit the device together. Methods for identifying and quantifying metabolites and lipids from cell lysates continue to improve with automated extractions, chromatographic separations, and advances in mass spectrometer sensitivity and resolution.

Single-cell technologies are a natural extension of the bulk analyses mentioned above, using analyte enrichment and signal amplification to quantify heterogeneity in transcript regulation and protein expression in a cell population. These datasets are markedly different from ensemble averages from bulk analyses and are much more expensive to produce. As technology advances, single-cell analysis costs should decrease to the level of current screening tools. These single-cell analyses promise to further enhance the power of personalized medicine, currently enabled by -omics approaches that provide ensemble datasets.

Cell-containing scaffolds for generating scalable tissue- and organ-on-demand structures

The barriers to adopting alternative culture methods and moving beyond monolayers on plasticware are numerous and valid. To address these challenges, we and others retained the ease of pipetting cell suspensions into a well plate by using pre-formed porous scaffolds. These scaffolds have a defined volume and readily support cell-laden hydrogels delivered *via* a micropipette.[84–86] Our work builds on the paper scaffolds described by Whitesides.[87] Other prominent scaffold materials include silk fibroin,[88] crosslinked proteins from human platelet lysates,[89] and polymer blends of poly(ε-caprolactone), poly (ethylene glycol), and polylactic acid.[90–92] Recently, we described an open-well scaffold free of fibers, enabling easier microscopic analysis of cell-laden hydrogels without fixation or optical clearing.[93,94] These well-like structures were prepared by attaching laser-cut silicone to a porous polyethylene terephthalate (PET) sheet. The PET sheet retained the gel slab while allowing the exchange of nutrients and signaling molecules with the culture medium.

Pre-formed porous scaffolds meet the three aspects we believe are necessary for a successful OoC device. For example, many *anatomically relevant tissue structures* have been generated with paper-based scaffolds, including a recently described origami-folded cardiac tissue,[95] a kidney proximal tubule model,[96] a liver model containing hepatocytes and non-parenchymal cells,[97] and a multi-organ platform combining 3D-printed devices and paper scaffolds.[98] Progress in culture complexity has also continued with other scaffold-based cultures, with organ-level systems constructed by stacking scaffolds or integrating them into 3D-printed devices. We have used paper scaffolds to quantify cellular invasion,[99–102] drug metabolism in tumor-like structures,[103,104] estrogen signaling in mammary tissue models,[43,105,106] and phase I and II drug metabolism in hepatocytes maintained under physiologically appropriate oxygen tensions.[107,108] One admitted limitation of this approach is the reliance on commercial vendors for scaffold materials, which limits our ability to tailor their physicochemical properties. Despite this, the success of our work and that of many others in generating paper-based microfluidic devices, point-of-care diagnostics, and culture platforms suggests that available options are sufficient to meet most needs.[109–112]

The *ease of sample collection* from paper and other porous scaffolds matches that of other ECM-rich cell cultures, including those maintained in well plates or microfluidic channels. To free cells from scaffolds, the ECM is enzymatically degraded or cooled until it returns to a liquid state. To collect cell contents, standard lysis procedures and downstream sample cleanup are performed with commercial kits. The thickness or diameter of circular scaffolds can be easily scaled to provide the number of cells needed for the readouts listed in Table 1. This approach also maintains a similar cell/ECM density across different scaffold sizes. These sorts of changes can be rapidly prototyped using scissors, folding, or other accessible methods. Maintaining a consistent cell density within a scaffold is important for generating reproducible datasets and avoiding differences in pericellular hypoxia. McGuigan and colleagues established a cellulose scaffold-based system (TRACER) for spatially resolved analysis of cell behavior supported on a single-piece scaffold.[113] This platform supports confocal analysis with cell fixation and staining, RNA collection for PCR, and analysis of rapidly changing metabolites by MS. McGuigan and colleagues have continued to advance orga-

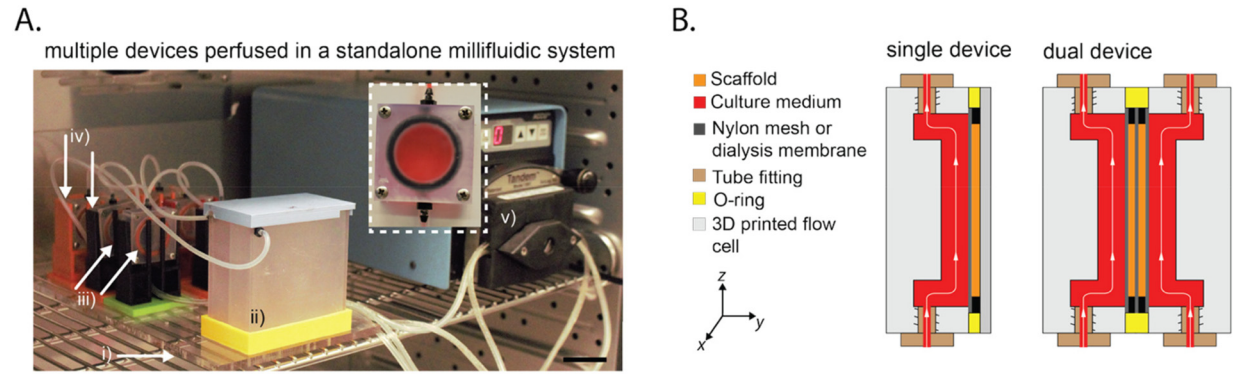

Fig. 4 A continuous-flow culture system developed in our laboratory, capable of perfusing cell-laden scaffolds. Adapted from ref. 116, copyright 2024, with permission from the RSC. (A) A photograph of the assembled millifluidic system, which consists of (i) an acrylic base, (ii) a 3D printed medium reservoir, (iii) 3D printed flow devices, (iv) device holders to ensure they remained upright throughout an experiment, and (v) a peristaltic pump. The inset is a photograph of an assembled device filled with a red food-coloring solution. (B) Schematics of a (left) single and (right) dual device structure, where each device can perfuse a single paper scaffold or multiple stacked into a tissue- or organ-like structure.

noid preparation and automation with their SPOT platform.[114] We have demonstrated the ability to quantify drug metabolites extracted from paper scaffolds using a targeted LC-MS approach.[104] We have further demonstrated the compatibility of confocal microscopy for investigating ERα in T47D cells under hypoxic and normoxic conditions.[106] Collectively, these studies showcase that scaffold-based 3D culture systems can bridge the gap between physiologically relevant tissue architecture and practical experimental accessibility, enabling spatially resolved, multi-modal analysis of cellular function while remaining compatible with established workflows.

There are few *continuous perfusion systems* in which preformed scaffolds are supplied with new medium. For example, Fu described a paper device that used capillary action to draw culture medium from a reservoir, along a paper strip, to a region containing a cell-laden hydrogel.[115] After wetting the strip and cell region, the medium and nutrients flowed through the strips by capillary action. We recently described a device (Fig. 4A) that passes culture medium through 3D-printed holders containing cell-laden scaffolds.[116] These holders can accommodate scaffolds of various diameters or thicknesses, offering modularity and a platform for analysis using already developed protocols. The two-chamber holder depicted in Fig. 4B allows simultaneous perfusion of two distinct cell populations. These chambers are separated by a porous membrane that prevents physical contact while allowing intercellular signaling. This system recirculates medium from a central reservoir, providing a steady nutrient supply to the cells. Tubeless systems, like those described by Pompano and others,[75,76] are compact, standalone units that provide small experimental footprints. We envision future iterations of the continuous flow device having a fluid-exchange mechanism that eliminates tubing and incorporates sampling ports to introduce an NCE or collect a sample mid-experiment.

We strive to advance a culture format that bridges the gap between the inaccurate yet widely popular monolayer format and highly complex, less accessible OoC devices. By leveraging the maker movement, paper scaffolds and 3D printing can be used to generate modular systems. Laboratories can adapt these systems to their specific needs, while retaining the key features outlined above. Readily accessible devices will likely not—and in some cases should not—replace highly engineered OoC systems, but they aim to transition laboratories to more advanced culture practices that balance physiological relevance with practicality and accessibility.

Increased acceptance and adoption of NAMs is through standardization and detailed experimental evaluation

The current regulatory framework for assessing and accepting NAMs is thorough.[117] The time it takes to generate a publishable device prototype or dataset seems instantaneous compared to the glacial pace of regulatory evaluation of a single NAM. Better regulatory guidance for the research laboratory and funding for independently organized interlaboratory comparisons could more quickly determine the technology readiness level before submission to regulators. In 2021, Piergiovanni outlined the gap between current reporting and testing levels and the need to assess NAM functionality.[118] We argue that a framework is needed to address this gap within the research laboratory, with (1) defined libraries of NCEs under similar dosing conditions and (2) funding for large-scale studies to ensure inter-laboratory reproducibility. There are currently no such standards for monolayer or 3D cultures, with many laboratories adopting protocols that best match their workflows and constraints.

A practical path forward for many OoC devices is a defined metric, one that evaluates a library of known NCEs that failed (or succeeded) in pre-clinical and clinical trials. These evaluations should be run in parallel with monolayer cultures. Comparisons with responses in monolayers are not the goal of

NAMs, given their inherent lack of predictive power. Monolayer cultures serve as an important benchmark, demonstrating a lab's ability to reproduce results under defined culture conditions. OoC devices often have different cell densities or ECM-rich environments, making it difficult to disentangle artifacts arising from non-standard laboratory practices. The National Institutes of Health LiverTox database catalogs drug-induced liver injury caused by prescription and nonprescription medicines,[119] and serves as a resource for evaluating the predictive power of any liver-related NAM. With an established protocol, the next confirmation of utility is an intra-laboratory one, in which researchers at different stages of training repeat experiments and compare datasets. The reproducibility of these datasets will determine NAM's technology readiness level and its potential for larger, interlaboratory comparisons. In parallel, a comprehensive and easily searchable database is needed for the NAMs community to compare predicted outcomes and *ease of sample collection* across endpoint and -omics-level studies. Only with this larger support structure can we collectively address the goal of the FDA Modernization Act 2.0 and answer, "*If two devices have similar predictive power, which aspects are more amenable to broad adoption?*".

Concluding thoughts

The input and efforts of analytical chemists in (1) the development and validation of NAMs and (2) the fabrication and evaluation of OoC devices are critical. Whether assembled using advanced fabrication techniques or makerspace tools, predictive power relies on accurate measurements of cellular responses to NCEs with known outcomes. As with traditional culture formats, there is no one-size-fits-all means of assessing these cellular responses. Current approaches for fabricating tissue- and organ-like cultures in micro- and millifluidic devices can be categorized broadly as: (1) μTAS devices requiring limited user input once cells and ECM are placed in the appropriate places, and (2) construction of fit-for-purpose devices using readily accessible materials and laboratory tools in a do-it-yourself manner. The increasing availability of additive manufacturing technologies and tools that can fabricate parts by laser cutting bulk materials makes microfabricated devices and chips available to all laboratories. Regardless of the fabrication method, the main challenges remain increasing anatomical and physiological relevance, introducing controlled perfusion for nutrient and waste exchange, and improving technical practicality by making it easier to obtain the samples needed for quantitative measurements. We believe a successful path forward is two-fold: (1) a roadmap by which all tools are benchmarked and datasets compared to determine the strengths and weaknesses of current and future approaches, and (2) a series of tools that provide meaningful datasets with low barriers of entry for traditional cell culture laboratories. By creating these benchmarks, a more accessible foundation can be established for laboratories to enter the realm of microfluidics. While we have not reached the destination, the path forward is becoming increasingly clear.

Conflicts of interest

There are no conflicts to declare.

Data availability

This perspective contains no new datasets but rather highlights important work being done in the field. All images in the Perspective were from already published sources, and permissions for usage were obtained. There are no new datasets or reanalysis of previously published work.

Acknowledgements

This work was supported by the National Institute of General Medical Sciences through Grant Award Number R35 GM128697 and the National Institute of Environmental Health Sciences through Grant Award Number R01 ES032730.

References

1 J. J. Han, FDA Modernization Act 2.0 allows for alternatives to animal testing, *Artif. Organs*, 2023, **47**(3), 449–450, DOI: 10.1111/aor.14503.
2 D. Sun, W. Gao, H. Hu and S. Zhou, Why 90% of clinical drug development fails and how to improve it?, *Acta Pharm. Sin. B*, 2022, **12**(7), 3049–3062, DOI: 10.1016/j.apsb.2022.02.002.
3 D. A. Tagle, The NIH microphysiological systems program: developing in vitro tools for safety and efficacy in drug development, *Curr. Opin. Pharmacol.*, 2019, **48**(1), 146–154, DOI: 10.1016/j.coph.2019.09.007.
4 I. J. Onakpoya, C. J. Heneghan and J. K. Aronson, Post-marketing withdrawal of 462 medicinal products because of adverse drug reactions: a systematic review of the world literature, *BMC Med.*, 2016, **14**, 10, DOI: 10.1186/s12916-016-0553-2.
5 A. Sertkaya, T. Beleche, A. Jessup and B. D. Sommers, Costs of drug development and research and development intensity in the US, 2000–2018, *JAMA Network Open*, 2024, **7**(6), e2415445, DOI: 10.1001/jamanetworkopen.2024.15445.
6 R. M. Sutherland, J. A. McCredie and W. R. Inch, Growth of multicell spheroids in tissue culture as a model of nodular carcinomas, *J. Natl. Cancer Inst.*, 1971, **46**(1), 113–120.
7 R. L. Sutherland, W. R. Inch, J. A. McCredie and J. Kruuv, Multi-component radiation survival curve using an *in vitro* tumour model, *Int. J. Radiat. Biol. Relat. Stud. Phys., Chem. Med.*, 1970, **18**(5), 491–495.

8 M. J. Bissell, A. Rizki and I. S. Mian, Tissue architecture: The ultimate regulator of breast epithelial function, *Curr. Opin. Cell Biol.*, 2003, **15**(6), 753–762, DOI: 10.1016/j.ceb.2003.10.016.
9 V. Weaver, A. Fischer, O. Peterson and M. Bissell, The importance of the microenvironment in breast cancer progression: Recapitulation of mammary tumorigenesis using a unique human mammary epithelial cell model and a three-dimensional culture assay, *Biochem. Cell Biol.*, 1996, **74**(6), 833–851, DOI: 10.1139/o96-089.
10 H. G. Hall, D. A. Farson and M. J. Bissell, Lumen formation by epithelial-cell lines in response to collagen overlay: A morphogenetic model in culture, *Proc. Natl. Acad. Sci. U. S. A.*, 1982, **79**(15), 4672–4676, DOI: 10.1073/pnas.79.15.4672.
11 Z. Živković and T. Opačak-Bernardi, An overview on spheroid and organoid models in applied studies, *Science*, 2025, **7**(1), 27, DOI: 10.3390/sci7010027.
12 D. Singh, A. Thakur, Rakesh and A. Kumar, Advancements in organoid-based drug discovery: Revolutionizing precision medicine and pharmacology, *Drug Dev. Res.*, 2025, **86**(4), e70121, DOI: 10.1002/ddr.70121.
13 G. Fang, Y. C. Chen, H. Lu and D. Jin, Advances in spheroids and organoids on a chip, *Adv. Funct. Mater.*, 2023, **33**(19), 2215043, DOI: 10.1002/adfm.202215043.
14 E. Järvinen, H. S. Hammer, O. Pötz, M. Ingelman-Sundberg and T. B. Stage, 3D spheroid primary human hepatocytes for prediction of cytochrome P450 and drug transporter Induction, *Clin. Pharmacol. Ther.*, 2023, **113**(6), 1284–1294, DOI: 10.1002/cpt.2887.
15 M. Ingelman-Sundberg and V. Lauschke, 3D human liver spheroids for translational pharmacology and toxicology, *Basic Clin. Pharmacol. Toxicol.*, 2022, **130**, 5–15, DOI: 10.1111/bcpt.13587.
16 G. Mehta, A. Y. Hsiao, M. Ingram, G. D. Luker and S. Takayama, Opportunities and challenges for use of tumor spheroids as models to test drug delivery and efficacy, *J. Controlled Release*, 2012, **164**(2), 192–204, DOI: 10.1016/j.jconrel.2012.04.045.
17 X. Liu and A. B. Hummon, Mass spectrometry imaging of therapeutics from animal models to three-dimensional cell cultures, *Anal. Chem.*, 2015, **87**(19), 9508–9519, DOI: 10.1021/acs.analchem.5b00419.
18 D. Huh, B. D. Matthews, A. Mammoto, M. Montoya-Zavala, H. Y. Hsin and D. E. Ingber, Reconstituting organ-level lung functions on a chip, *Science*, 2010, **328**(5986), 1662–1668, DOI: 10.1126/science.1188302.
19 J. Vetter, I. Palagi, A. Waisman and A. Blaeser, Recent advances in blood-brain barrier-on-a-chip models, *Acta Biomater.*, 2025, **197**(1), 1–28, DOI: 10.1016/j.actbio.2025.03.041.
20 A. Valiei, J. Aminian-Dehkordi and M. R. K. Mofrad, Gut-on-a-chip models for dissecting the gut microbiology and physiology, *APL Bioeng.*, 2023, **7**(1), 011502, DOI: 10.1063/5.0126541.
21 W. Huang, Y. Y. Chen, F. F. He and C. Zhang, Revolutionizing nephrology research: expanding horizons with kidney-on-a-chip and beyond, *Front. Bioeng. Biotechnol.*, 2024, **12**, 1373386, DOI: 10.3389/fbioe.2024.1373386.
22 L. Qiu, B. Kong, T. Kong and H. Wang, Recent advances in liver-on-chips: Design, fabrication, and applications, *Smart Med.*, 2023, **2**(1), e20220010, DOI: 10.1002/SMMD.20220010.
23 A. I. Morrison, M. J. Sjoerds, L. A. Vonk, S. Gibbs and J. J. Koning, In vitro immunity: an overview of immunocompetent organ-on-chip models, *Front. Immunol.*, 2024, **15**, 1373186, DOI: 10.3389/fimmu.2024.1373186.
24 Y. Kim, H. Kim and Y. Kim, Advancing hepatotoxicity assessment: current advances and future directions, *Toxicol. Res.*, 2025, **41**(4), 303–323, DOI: 10.1007/s43188-025-00289-w.
25 R. G. Harrison, The outgrowth of the nerve fiber as a mode of protoplasmic movement, *J. Exp. Zool.*, 1910, **34**(3), 243–256, DOI: 10.1002/jez.1400090405.
26 A. Carrel and M. T. Burrows, Cultivation of tissues in vitro and its technique, *J. Exp. Med.*, 1911, **13**(3), 387–396, DOI: 10.1084/jem.13.3.387.
27 W. F. Scherer, J. T. Syverton and G. O. Gey, Studies on the propagation in vitro of poliomyelitis viruses, *J. Exp. Med.*, 1953, **97**(5), 695–710.
28 C. Hirsch and S. Schildknecht, In vitro research reproducibility: Keeping up high standards, *Front. Pharmacol.*, 2019, **10**, 1484, DOI: 10.3389/fphar.2019.01484.
29 T. M. Errington, A. Denis, N. Perfito, E. Iorns and B. A. Nosek, Challenges for assessing replicability in preclinical cancer biology, *eLife*, 2021, **10**, e67995, DOI: 10.7554/eLife.67995.
30 S. A. Bustin, V. Benes, J. A. Garson, J. Hellemans, J. Huggett, M. Kubista, R. Mueller, T. Nolan, M. W. Pfaffl, G. L. Shipley, *et al.*, The MIQE guidelines: Minimum information for publication of quanitative real-time PCR experiments, *Clin. Chem.*, 2009, **55**(4), 611–622.
31 S. A. Bustin, J. M. Ruijter, M. J. B. van den Hoff, M. Kubista, M. W. Pfaffl, G. L. Shipley, S. Rödiger, A. Untergasser, R. Mueller, T. Nolan, *et al.*, MIQE 2.0: Revision of the minimum information for publication of quantitative real-time PCR experiments guidelines, *Clin. Chem.*, 2025, **71**(6), 634–651, DOI: 10.1093/clinchem/hvaf043.
32 T. Riss, R. Moravec, S. Duellman and A. Niles, Treating cells as reagents to design reproducible assays, *SLAS Discovery*, 2021, **26**(10), 1256–1267, DOI: 10.1177/24725552211039754.
33 Z. R. Sitte, T. S. Larson, J. C. McIntosh, M. Sinanian and M. R. Lockett, Selecting the appropriate indirect viability assay for 3D paper-based cultures: a data-driven study, *Analyst*, 2023, **148**(10), 2245–2255, DOI: 10.1039/d3an00283g.
34 M. W. Boyce, R. M. Kenney, A. S. Truong and M. R. Lockett, Quantifying oxygen in paper-based cell cul-

tures with luminescent thin film sensors, *Anal. Bioanal. Chem.*, 2016, **408**(11), 2985–2992, DOI: 10.1007/s00216-015-9189-x.

35 R. M. Kenney, M. W. Boyce, N. A. Whitman, B. P. Kromhout and M. R. Lockett, A pH-sensing optode for mapping spatiotemporal gradients in 3D paper-based cell cultures, *Anal. Chem.*, 2018, **90**(3), 2376–2383, DOI: 10.1021/acs.analchem.7b05015.

36 K. R. Rivera, M. A. Yokus, P. D. Erb, V. A. Pozdin and M. Daniele, Measuring and regulating oxygen levels in microphysiological systems: design, material, and sensor considerations, *Analyst*, 2019, **144**(10), 3190–3215, DOI: 10.1039/c8an02201a.

37 Y. Huang, T. Liu, Q. Huang and Y. Wang, From organ-on-a-chip to human-on-a-chip: A review of research progress and latest applications, *ACS Sens.*, 2024, **9**(7), 3466–3488, DOI: 10.1021/acssensors.4c00004.

38 Y. Wang, X. Chang, S. Deng, S. Tang and P. Chen, Functional material probes and advanced technologies in organ-on-a-chip characterization, *Theranostics*, 2026, **16**(5), 2488–2516, DOI: 10.7150/thno.122552.

39 H. Kutluk, E. E. Bastounis and I. Constantinou, Integration of extracellular matrices into organ-on-chip systems, *Adv. Healthcare Mater.*, 2023, **12**(20), e2203256, DOI: 10.1002/adhm.202203256.

40 N. L. Stone, T. J. England and S. E. O'Sullivan, A novel transwell blood brain barrier model using primary human cells, *Front. Cell. Neurosci.*, 2019, **13**, 230, DOI: 10.3389/fncel.2019.00230.

41 R. M. Kenney, C. C. Lloyd, N. A. Whitman and M. R. Lockett, 3D cellular invasion platforms: How do paper-based cultures stack up?, *Chem. Commun.*, 2017, **53**(53), 7194–7210, DOI: 10.1039/c7cc02357j.

42 R. M. Kenney, A. Loeser, N. A. Whitman and M. R. Lockett, Paper-based Transwell assays: An inexpensive alternative to study cellular invasion, *Analyst*, 2019, **144**(1), 206–211, DOI: 10.1039/c8an01157e.

43 Z. R. Sitte, A. A. Miranda Buzetta, S. J. Jones, Z. W. Lin, N. A. Whitman and M. R. Lockett, Paper-based coculture platform to evaluate the effects of fibroblasts on estrogen signaling in ER+ breast cancers, *ACS Meas. Sci. Au*, 2023, **3**(6), 479–487, DOI: 10.1021/acsmeasuresciau.3c00032.

44 C. Konig and A. Runge, Metastatic dissemination mimicked in a multicellular transwell assay, *Methods Mol. Biol.*, 2021, **2235**(1), 181–190, DOI: 10.1007/978-1-0716-1056-5_13.

45 M. Del Nero, A. Colombo, S. Garbujo, C. Baioni, L. Barbieri, M. Innocenti, D. Prosperi, M. Colombo and L. Fiandra, Advanced cell culture models illuminate the interplay between mammary tumor cells and activated fibroblasts, *Cancers*, 2023, **15**(9), 2498, DOI: 10.3390/cancers15092498.

46 P. Dalsbecker, S. Suominen, M. A. Faridi, R. Mahdavi, J. Johansson, C. H. Blomqvist, M. Goksör, K. Aalto-Setälä, L. E. Viiri and C. B. Adiels, An in vivo mimetic liver-lobule-chip (LLoC) for stem cell maturation, and zonation of hepatocyte-like cells on chip, *Lab Chip*, 2025, **25**(17), 4328–4344, DOI: 10.1039/d4lc00509k.

47 M. Watanabe, A. Salvadori, M. Markovic, R. Sudo and A. Ovsianikov, Advanced liver-on-chip model mimicking hepatic lobule with continuous microvascular network via high-definition laser patterning, *Mater. Today Bio*, 2024, **32**(1), 1015643, DOI: 10.1016/j.mtbio.2025.101643.

48 S. Park and E. W. K. Young, E-FLOAT: Extractable Floating Liquid gel-based Organ-on-a-chip for Airway Tissue modeling under airflow, *Adv. Mater. Technol.*, 2021, **6**(12), 2100828, DOI: 10.1002/admt.202100828.

49 T. Weigel, C. Malkmus, V. Weigel, M. Wußmann, C. Berger, J. Brennecke, F. Groeber-Becker and J. Hansmann, Fully synthetic 3D fibrous scaffolds for stromal tissues-replacement of animal-derived scaffold materials demonstrated by multilayered skin, *Adv. Mater.*, 2022, **34**(10), e2106780, DOI: 10.1002/adma.202106780.

50 J. Vajda, M. Milojević, U. Maver and B. Vihar, Microvascular tissue engineering—A review, *Biomedicines*, 2021, **9**(6), 589, DOI: 10.3390/biomedicines9060589.

51 V. Palacio-Castaneda, N. Velthuijs, S. Le Gac and W. P. R. Verdurmen, Oxygen control: The often overlooked but essential piece to create better in vitro systems, *Lab Chip*, 2022, **22**(6), 1068–1092, DOI: 10.1039/d1lc00603g.

52 T. Place, F. Domann and A. Case, Limitations of oxygen delivery to cells in culture: An underappreciated problem in basic and translational research, *Free Radicals Biol. Med.*, 2017, **113**, 311–322, DOI: 10.1016/j.freeradbiomed.2017.10.003.

53 G. L. Semenza, Oxygen sensing, hypoxia-inducible factors, and disease pathophysiology, *Annu. Rev. Pathol.: Mech. Dis.*, 2014, **9**(1), 47–71, DOI: 10.1146/annurev-pathol-012513-104720.

54 E. A. Sheta, H. Trout, J. J. Gildea, M. A. Harding and D. Theodorescu, Cell density mediated pericellular hypoxia leads to induction of HIF-1a via nitric oxide and Ras/MAP kinase mediated signaling pathways, *Oncogene*, 2001, **20**(52), 7624–7634, DOI: 10.1038/sj.onc.1204972.

55 J. Chiche, M. C. Brahimi-Horn and J. Pouyssegur, Tumor hypoxia induces a metabolic shift causing acidosis: A common feature in cancer, *J. Cell. Mol. Med.*, 2010, **14**(4), 771–794.

56 G. LaMonte, X. Tang, J. L. Y. Chen, J. Wu, C. H. C. Ding, M. M. Keenan, C. Sangokoya, H. N. Kung, O. Ilkayeva, L. G. Boros, *et al.*, Acidosis induces reprogramming of cellular metabolism to mitigate oxidative stress, *Cancer Metab.*, 2013, **1**, 23, DOI: 10.1186/2049-3002-1-23.

57 M. Azimzadeh, P. Khashayar, M. Amereh, N. Tasnim, M. Hoorfar and M. Akbari, Microfluidic-based oxygen (O2) sensors for on-chip monitoring of cell, tissue and organ metabolism, *Biosensors*, 2021, **12**(1), 6, DOI: 10.3390/bios12010006.

58 S. Banik, A. Uchil, T. Kalsang, S. Chakrabarty, M. A. Ali, P. Srisungsitthisunti, K. K. Mahato, S. Surdo and N. Mazumber, The revolution of PDMS microfluidics in

cellular biology, *Crit. Rev. Biotechnol.*, 2023, **43**(3), 465–483, DOI: 10.1080/07388551.2022.2034733.

59 C. J. Ochs, J. Kasuya, A. Pavesi and R. D. Kamm, Oxygen levels in thermoplastic microfluidic devices during cell culture, *Lab Chip*, 2014, **14**(3), 459–462, DOI: 10.1039/c3lc51160j.

60 S. Zips, L. Hiendlmeier, L. J. K. Weiß, H. Url, T. F. Teshima, R. Schmid, M. Eblenkamp, P. Mela and B. Wolfrum, Biocompatible, flexible, and oxygen-permeable silicone-hydrogel material for stereolithographic printing of microfluidic lab-on-a-chip and cell-culture devices, *ACS Appl. Polym. Mater.*, 2020, **3**(1), 243–258, DOI: 10.1021/acsapm.0c01071.

61 L. Sønstevold, P. Koza, M. Czerkies, E. Andreassen, P. McMahon and E. Vereshchagina, Prototyping in polymethylpentene to enable oxygen-permeable on-a-chip cell culture and organ-on-a-chip devices suitable for microscopy, *Micromachines*, 2024, **15**(7), 898, DOI: 10.3390/mi15070898.

62 H. Lu, W. C. M. Wang, D. A. Lauffenburger, L. G. Griffith and K. F. Jensen, Microfluidic shear devices for quantitative analysis of cell adhesion, *Anal. Chem.*, 2004, **76**(8), 5257–5264.

63 K. M. Saqr, S. Tupin, S. Rshad, T. Endo, K. Niizuma, T. Tominaga and M. Ohta, Physiologic blood flow is turbulent, *Sci. Rep.*, 2020, **10**(1), 15492, DOI: 10.1038/s41598-020-72309-8.

64 N. Baeyens, C. Bandyopadhyay, B. G. Coon, S. Yun and M. A. Schwartz, Endothelial fluid shear stress sensing in vascular health and disease, *J. Clin. Invest.*, 2016, **126**(3), 821–828, DOI: 10.1172/JCI83083.

65 C. Luk, N. J. Haywood, K. I. Bridge and M. T. Kearney, Paracrine role of the endothelium in metabolic homeostasis in health and nutrient excess, *Front. Cardiovasc. Med.*, 2022, **9**(1), 882923, DOI: 10.3389/fcvm.2022.882923.

66 C. J. Mandrycky, C. C. Howard, S. G. Rayner, Y. J. Shin and Y. Zheng, Organ-on-a-chip systems for vascular biology, *J. Mol. Cell. Cardiol.*, 2022, **159**(1), 1–13, DOI: 10.1016/j.yjmcc.2021.06.002.

67 L. Xing, B. Liu, H. Wu, X. Wu, X. L. Wang, Y. Song, S. S. Zhang, J. Q. Li, L. Bi and G. Pei, The effect of fluid shear stress on fibroblasts and stem cells on plane and groove topographies, *Cell Adhes. Migr.*, 2020, **14**(1), 12–22, DOI: 10.1080/19336918.2020.1713532.

68 Z. D. Shi and J. M. Tarbell, Fluid flow mechanotransduction in vascular smooth muscle cells and fibroblasts, *Ann. Biomed. Eng.*, 2011, **39**(6), 1608–1619, DOI: 10.1007/s10439-011-0309-2.

69 C. K. Cheng, N. Wang, L. Wang and Y. Huang, Biophysical and biochemical roles of shear stress on endothelium: A revisit and new insights, *Circ. Res.*, 2025, **126**(7), 752–772, DOI: 10.1161/CIRCRESAHA.124.325685.

70 F. Zhang, D. S. Y. Lin, S. Rajasekar, A. Sorta and B. Zhang, Pump-less platform enables long-term recirculating perfusion of 3D printed tubular tissues, *Adv. Healthcare Mater.*, 2023, **12**(27), e2300423, DOI: 10.1002/adhm.202300423.

71 Y. I. Wang and M. L. Shuler, UniChip enables long-term recirculating unidirectional perfusion with gravity-driven flow for microphysiological systems, *Lab Chip*, 2018, **18**(17), 2563–2574, DOI: 10.1039/c8lc00394g.

72 M. Ansarizadeh, H. T. Nguyen, B. Lazovic, J. Kettunen, L. De Silva, R. Sivakumar, P. Junttila, S. L. Rissanen, R. Hicks, P. Singh, *et al.*, Microfluidic vessel-on-chip platform for investigation of cellular defects in venous malformations and responses to various shear stress and flow conditions, *Lab Chip*, 2025, **25**(4), 613–630, DOI: 10.1039/d4lc00824c.

73 M. A. Skylar-Scott, S. G. M. Uzel, L. L. Nam, J. H. Ahrens, R. L. Truby, S. Damaraju and J. A. Lewis, Biomanufacturing of organ-specific tissues with high cellular density and embedded vascular channels, *Sci. Adv.*, 2019, **5**(9), 1–13, DOI: 10.1126/sciadv.aaw2459.

74 S. W. Chen, A. Blazeski, S. Zhang, S. E. Shelton, G. S. Offeddu and R. D. Kamm, Development of a perfusable, hierarchical microvasculature-on-a-chip model, *Lab Chip*, 2023, **23**(20), 4552–4564, DOI: 10.1039/d3lc00512g.

75 S. R. Cook, E. E. Lawrence, P. Sakinejad and R. R. Pompano, Open-source tubing-free impeller pump platform for controlled recirculating fluid flow for microfluidics and organs-on-chip, *HardwareX*, 2025, **23**, e00673, DOI: 10.1016/j.ohx.2025.e00673.

76 S. R. Cook, A. G. Ball, A. Mohammad and R. R. Pompano, A 3D-printed multi-compartment organ-on-chip platform with a tubing-free pump models communication with the lymph node, *Lab Chip*, 2025, **25**(2), 155–174, DOI: 10.1039/d4lc00489b.

77 S. Ning, S. Liu, Y. Xiao, G. Zhang, W. Cui and M. Reed, A microfluidic chip with a serpentine channel enabling high-throughput cell separation using surface acoustic waves, *Lab Chip*, 2021, **21**(23), 4608–4617, DOI: 10.1039/d1lc00840d.

78 S. Shen, L. Zhao, H. Bai, Y. Zhang, Y. Niu, C. Tian and H. Chan, Spiral large-dimension microfluidic channel for flow-rate- and particle-size-insensitive focusing by the stabilization and acceleration of secondary flow, *Anal. Chem.*, 2024, **96**(4), 1750–1758, DOI: 10.1021/acs.analchem.3c04897.

79 C. W. Kan, C. I. Tobos, D. M. Rissin, A. D. Wiener, R. E. Meyer, D. M. Svancara, A. Comperchio, C. Warwick, R. Millington, N. Collier, *et al.*, Digital enzyme-linked immunosorbent assays with sub-attomolar detection limits based on low numbers of capture beads combined with high efficiency bead analysis, *Lab Chip*, 2020, **20**(12), 2122–2135, DOI: 10.1039/d0lc00267d.

80 S. Zhang, A. Garcia-D'Angeli, J. P. Brennan and Q. Huo, Predicting detection limits of enzyme-linked immunosorbent assay (ELISA) and bioanalytical techniques in general, *Analyst*, 2014, **139**(2), 439–445, DOI: 10.1039/c3an01835k.

81 E. Grigorov, B. Kirov, M. B. Marinov and V. Galabov, Review of microfluidic methods for cellular lysis, *Micromachines*, 2021, **12**(5), 498, DOI: 10.3390/mi12050498.
82 S. Taylor, M. Wakem, G. Dijkman, M. Alsarraj and M. Nguyen, A practical approach to RT-qPCR-Publishing data that conform to the MIQE guidelines, *Methods*, 2010, **50**(4), S1–S5, DOI: 10.1016/j.ymeth.2010.01.005.
83 *Bioinformatics for Beginners*, National Cancer Institute Center for Cancer Research, 2022. https://bioinformatics.ccr.cancer.gov/docs/b4b/RNASeq_Overview/02.Sample_Prep/ (accessed 2025 12.08).
84 M. Chakraborty and A. Devi, Landscape of scaffolds from advanced synthesis to tissue engineering, *Mater. Today Chem.*, 2024, **40**, 102258, DOI: 10.1016/j.mtchem.2024.102258.
85 K. Peranidze, N. S. Yadavalli, B. Blevins, M. Parker, T. Jain, M. Aghajohari, S. Minko and V. Reukov, Strategies for fabricating aligned nano- and microfiber scaffolds: an overview for cell culture applications, *Nanoscale*, 2025, **17**(36), 20670–20703, DOI: 10.1039/d5nr02078f.
86 S. M. Cramer, T. S. Larson and M. R. Lockett, Tissue Papers: Leveraging paper-based microfluidics for the next generation of 3D tissue models, *Anal. Chem.*, 2019, **91**(17), 10916–10926, DOI: 10.1021/acs.analchem.9b02102.
87 R. Derda, A. Laromaine, A. Mammoto, S. K. Tang, T. Mammoto, D. E. Ingber and G. M. Whitesides, Paper-supported 3D cell culture for tissue-based bioassays, *Proc. Natl. Acad. Sci. U. S. A.*, 2009, **106**(44), 18457–18462, DOI: 10.1073/pnas.0910666106.
88 L. Ma, W. Dong, E. Lai and J. Wang, Silk fibroin-based scaffolds for tissue engineering, *Front. Bioeng. Biotechnol.*, 2024, **12**, 1381838, DOI: 10.3389/fbioe.2024.1381838.
89 S. C. Santos, C. A. Custódio and J. F. Mano, Human protein-based porous scaffolds as platforms for xeno-free 3D cell culture, *Adv. Healthcare Mater.*, 2022, **11**(12), e2102383, DOI: 10.1002/adhm.202102383.
90 B. Sowmya, A. B. Hemavathi and P. K. Panda, Poly (ε-caprolactone)-based electrospun nano-featured substrate for tissue engineering applications: a review, *Prog. Biomater.*, 2021, **10**(2), 91–117, DOI: 10.1007/s40204-021-00157-4.
91 S. Castañeda-Rodríguez, M. González-Torres, R. M. Ribas-Aparicio, M. L. D. Prado-Audelo, G. Levya-Gómez, E. S. Gürer and J. Sharifi-Rad, Recent advances in modified poly (lactic acid) as tissue engineering materials, *J. Biol. Eng.*, 2023, **17**(1), 21, DOI: 10.1186/s13036-023-00338-8.
92 J. Zhu, Bioactive modification of poly(ethylene glycol) hydrogels for tissue engineering, *Biomaterials*, 2010, **13**(17), 4639–4656, DOI: 10.1016/j.biomaterials.2010.02.044.
93 Z. R. Sitte, E. E. Karlsson, T. S. Larson, H. Li, H. Zhou and M. R. Lockett, Supported gel slabs (SGS) scaffolds for generating tissue- and tumor-like environments on demand, *Analyst*, 2024, **149**(18), 4653–4662, DOI: 10.1039/D4AN00691G.
94 H. Dermutz, G. Thompson-Steckel, C. Forro, V. de Lange, L. Dorwling-Carter, J. Voros and L. Demko, Paper-based patterned 3D neural cultures as a tool to study network activity on multielectrode arrays, *RSC Adv.*, 2017, **7**(62), 39359–39371.
95 A. Sileo, F. Montrone, A. Rouchon, D. Trueb, J. Selvi, M. Schmid, F. Graef, G. Serino, D. Massai, N. Di Maggio, *et al.*, Toward origami-inspired in vitro cardiac tissue models, *ACS Biomater. Sci. Eng.*, 2025, **11**(3), 1583–1597, DOI: 10.1021/acsbiomaterials.4c01594.
96 H. Liu, G. M. Guo, Z. W. Yu, Y. L. Lin, C. H. Lin and M. M. Liu, A paper-based human kidney proximal tubule-on-a-chip for efficacy of SGLT2 inhibitors and methotrexate-induced nephrotoxicity assessment, *Biotechnol. J.*, 2025, **20**(8), e70099, DOI: 10.1002/biot.70099.
97 T. Agarwal, S. K. Biswas, S. Pal, T. K. Maiti, S. Chakraborty, S. K. Ghosh and R. Dhar, Inexpensive and versatile paper-based platform for 3D culture of liver cells and related bioassays, *ACS Appl. Bio Mater.*, 2020, **3**(4), 2522–2533, DOI: 10.1021/acsabm.0c00237.
98 H. Li, F. Cheng, Z. Wang, W. Li, J. A. Robledo-Lara and Y. S. Zhang, 3D-printed, configurable, paper-based, and autonomous multi-organ-on-paper platforms, *Mol. Syst. Des. Eng.*, 2022, **7**(11), 1538–1548, DOI: 10.1039/D2ME00142J.
99 R. M. Kenney, M. C. Lee, M. W. Boyce, Z. R. Sitte and M. R. Lockett, A cellular invasion assay for the real-time tracking of individual cells in spheroid or tumor-like mimics, *Anal. Chem.*, 2023, **95**(5), 3054–3061, DOI: 10.1021/acs.analchem.2p05201.
100 R. A. Lidgett, A. A. Miranda Buzetta, J. I. Baker, P. Dang, A. L. Oldenburg and M. R. Lockett, An analytical screening platform to differentiate acute and prolonged exposures of per- and polyfluoroalkyl substances on invasive cellular phenotypes, *Toxicol. Sci.*, 2025, **205**(2), 369–379, DOI: 10.1093/toxsci/kfaf044.
101 A. S. Truong, C. A. Lochbaum, M. W. Boyce and M. R. Lockett, Tracking the invasion of small numbers of cells in paper-based assays with quantitative PCR, *Anal. Chem.*, 2015, **87**(22), 11263–11270, DOI: 10.1021/acs.analchem.5b02362.
102 A. S. Truong and M. R. Lockett, Oxygen as a chemoattractant: confirming cellular hypoxia in paper-based invasion assays, *Analyst*, 2016, **141**(12), 3874–3882, DOI: 10.1039/C6AN00630B.
103 M. W. Boyce, G. J. LaBonia, A. B. Hummon and M. R. Lockett, Assessing chemotherapeutic effectiveness using a paper-based tumor model, *Analyst*, 2017, **142**(15), 2819–2827, DOI: 10.1039/c7an00806f.
104 T. S. Larson, G. L. Glish and M. R. Lockett, Spatially resolved quantification of drug metabolism and efficacy in 3D paper-based tumor mimics, *Anal. Chim. Acta*, 2021, **1186**, 339091, DOI: 10.1016/j.aca.2021.339091.

105 N. A. Whitman, Z. W. Lin, T. J. DiProspero, J. C. McIntosh and M. R. Lockett, Screening estrogen receptor modulators in a paper-based breast cancer model, *Anal. Chem.*, 2018, **90**(20), 11981–11988, DOI: 10.1021/acs.analchem.8b02486.

106 N. A. Whitman, Z. W. Lin, R. M. Kenney, L. Albertini and M. R. Lockett, Hypoxia differentially regulates estrogen receptor alpha in 2D and 3D culture formats, *Arch. Biochem. Biophys.*, 2019, **671**(1), 8–17, DOI: 10.1016/j.abb.2019.05.025.

107 T. J. Diprospero, L. G. Brown, T. D. Fachko and M. R. Lockett, Integration of physiological oxygen tensions and Wnt/B-catenin signaling into HepaRG cultures results in zonal patterning of drug metabolizing enzymes, *Drug Metab. Dispos.*, 2022, **50**(8), 1098–1105, DOI: 10.1124/dmd.122.000870.

108 T. J. DiProspero, E. Dalrymple and M. R. Lockett, Physiologically relevant oxygen tensions differentially regulate hepatotoxic responses in HepG2 cells, *Toxicol. In Vitro*, 2021, **74**, 105156, DOI: 10.1016/j.tiv.2021.105156.

109 T. Agarwal, M. Borrelli, P. Makvandi, M. Ashrafizadeh and T. Maiti, Paper-based cell culture: Paving the pathway for liver tissue model development on a cellulose paper chip, *ACS Appl. Bio Mater.*, 2020, **3**(7), 3956–3974, DOI: 10.1021/acsabm.0c00558.

110 K. Ng, B. Gao, K. W. Yong, Y. H. Li, M. Shi, X. Zhao, Z. D. Li, X. H. Zhang, B. Pingguan-Murphy, H. Yang, *et al.*, Paper-based culture platform and its emerging biomedical applications, *Mater. Today*, 2017, **20**(1), 32–44, DOI: 10.1016/j.mattod.2016.07.001.

111 S. C. Fernandes, J. A. Walz, D. J. Wilson, J. C. Brooks and C. R. Mace, Beyond wicking: Expanding the role of patterned paper as a foundation for an analytical platform, *Anal. Chem.*, 2017, **89**(11), 5654–5664.

112 E. Noviana, T. Ozer, C. S. Carrell, J. S. Link, C. McMahon, I. Jang and C. S. Henry, Microfluidic paper-based analytical devices: From design to applications, *Chem. Rev.*, 2021, **121**(19), 11835–11885, DOI: 10.1021/acs.chemrev.0c01335.

113 D. Rodenhizer, T. Dean, B. Xu, D. Cojocari and A. P. McGuigan, A three-dimensional engineered heterogeneous tumor model for assessing cellular environment and response, *Nat. Protoc.*, 2018, **13**(9), 1917–1957, DOI: 10.1038/s41596-018-0022-9.

114 R. Cao, N. T. Li, S. Latour, J. L. Cadavid, C. M. Tan, A. Forman, H. W. Jackson and A. P. McGuigan, An automation workflow for high-throughput manufacturing and analysis of scaffold-supported 3D tissue arrays, *Adv. Healthcare Mater.*, 2023, **12**(19), e2202422, DOI: 10.1002/adhm.202202422.

115 S. X. Fu, Z. Peng and B. C. Ye, A novel wick-like paper-based microfluidic device for 3D cell culture and anticancer drugs screening, *Biotechnol. J.*, 2021, **16**(2), 2000126, DOI: 10.1002/biot.202000126.

116 Z. R. Sitte, E. E. Karlsson, H. Li, H. Zhou and M. R. Lockett, A continuous flow device for laminar exchange of medium over cell-containing scaffolds and stacks, *Lab Chip*, 2024, **24**, 4105–4114, DOI: 10.1039/D4LC00480A.

117 G. Ouedraogo, N. Alépée, B. Tan and C. S. Roper, A call to action: Advancing new approach methodologies (NAMs) in regulatory toxicology through a unified framework for validation and acceptance, *Regul. Toxicol. Pharmacol.*, 2025, **162**, 105904, DOI: 10.1016/j.yrtph.2025.105904.

118 M. Piergiovanni, S. B. Leite and M. Whelan, Standardisation needs for organ on chip devices, *Lab Chip*, 2021, **21**(15), 2875–2868, DOI: 10.1039/D1LC00241D.

119 *LiverTox: Clinical and Research Information on Drug-Induced Liver Injury*. National Institute of Diabetes and Digestive and Kidney Diseases, 2012-. https://www.ncbi.nlm.nih.gov/books/NBK547852/ (accessed).